

Short-Circuit Diffusion in the Growth of Nickel Oxide Scales on Nickel Crystal Faces*

R. Herchl,† N. N. Khoi,† T. Homma,‡ and W. W. Smeltzer†

Received November 2, 1971—Revised January 6, 1972

A study has been made of the growth of nickel oxide layers on the (100), (110), and (111) crystal faces of nickel exposed to oxygen for periods up to 100 hr at temperatures in the range 500–800°C. These layers grow at a rate dependent upon the crystallographic orientation of the nickel face even at thicknesses within the scaling range. The (100) face oxidized more rapidly than the (110) and (111) nickel faces while the latter faces oxidized at different relative rates dependent upon temperature. A diffusional model is employed to interpret the oxidation kinetics wherein nickel transport proceeds in nickel oxide both by short-circuit diffusion at grain boundaries and by lattice diffusion.

INTRODUCTION

The kinetics for growth of the nickel oxide layer on nickel at temperatures within the range 400–600°C have been shown to be dependent upon structural properties of the oxide. Cathcart *et al.*¹ have recently advanced observations on the growth and mosaic structure of thin films up to 500 Å thick on several nickel faces to support the thesis that the oxidation rate is more rapid when the films contain larger densities of line defects and incoherent crystallite boundaries available for short-circuit diffusion of nickel. Perrow *et al.*^{2,3} have likewise demonstrated that these structural defects act as short-circuit diffusion paths in thicker films up to 8000 Å thick formed on polycrystalline nickel.

*This work forms part of a research program sponsored by the National Research Council of Canada.

†Department of Metallurgy and Materials Science, McMaster University, Hamilton, Ontario, Canada.

‡Present address: Institute of Industrial Science, University of Tokyo, Tokyo, Japan.

When polycrystalline nickel is exposed to oxygen at temperatures exceeding 500°C, investigators have obtained parabolic oxidation constants by taking tangents to the curves plotted according to the equation,

$$x^2 = K_p t + C \quad (1)$$

Here, x is the oxide layer thickness, K_p is the parabolic oxidation constant, t is the time, and C is a parameter dependent upon the scale thickness and time before onset of parabolic kinetics. Since the slope of the tangent (K_p) decreased with increasing exposure time, Gulbransen and Andrew⁴ suggested that this behavior could be possibly associated with grain boundary diffusion and since the oxide grains become larger as the layer thickens, the influence of grain boundary diffusion would finally become small compared to lattice diffusion. Results reported by Van der Broeck and Meijering⁵ corroborate this viewpoint since they have demonstrated that the evaluated parabolic constant is smaller when the oxide is "aged" by interrupted vacuum annealing cycles during an oxidation run. Also, Berry and Paidassi⁶ have shown that scaling curves for several grades of nickel over the large temperature range 600–1400°C when analyzed according to the parabolic equation exhibit an activation energy of 24 kcal/g atom up to 900°C and of 49–57 kcal/g-atom at temperatures exceeding 1000°C. The most accurate evaluation for the activation energy of nickel self-diffusion in a nickel oxide crystal is 61 kcal/g-atom.⁷ Thus, the activation energy for nickel oxide growth over the lower temperature range is but 0.4 the value for nickel lattice diffusion. All of these findings are consistent with the hypothesis that nickel transport across a growing oxide scale at intermediate temperatures involves an extensive degree of short-circuit diffusion.

To this time, a study has not been reported on the growth of scales on nickel crystal faces. In this communication, which forms part of a research program seeking correlations between metal oxidation kinetics and oxide structures, we report measurements on the growth of nickel oxide several microns thick on the (100), (110), and (111) crystal faces of nickel exposed to oxygen at temperatures in the range 500–800°C. It is demonstrated that oxidation controlled solely by lattice diffusion of nickel is not attained despite relatively long exposures extending to 100 hr. Accordingly, the results are analyzed in terms of a previously advanced model for oxide growth on metals wherein short-circuit diffusional properties play a predominant role in controlling reactant transport across a growing scale.³

EXPERIMENTAL

Using a spark cutter, specimens with desired orientations were cut as wafers approximately 1×10 mm in diameter from the single crystal boules of

99.999 wt % purity nickel supplied by Research Crystals Inc. Specimens were then given a vacuum anneal of 3×10^{-6} Torr at 900°C for 1 day. To prepare a specimen for oxidation by a gravimetric technique, it was mounted in bakelite and abraded on both sides with silicon carbide papers. This was followed by lapping on wheels impregnated with diamond paste of 6- and $1\text{-}\mu$ diameter, using kerosene as lubricant. The specimen was then removed from the mount and electropolished in 60% sulfuric acid aqueous solution maintained at 0°C under conditions of vigorous agitation to remove the damaged surface layer by dissolving up to $40\ \mu$ of nickel. Upon the removal of a specimen from the electropolishing bath, it was washed in distilled water and acetone. A given crystallographic orientation of a specimen surface was determined to within $\pm 2^\circ$ by the Laue back reflection x-ray technique. The edge area of a specimen accounted for less than 6% of the total surface area.

An assembly containing a Cahn RG continuously recording microbalance was used to determine the reaction kinetics of specimens exposed in a quartz tube to research grade oxygen at 400 Torr pressure and at temperatures within the range $500\text{--}800^\circ\text{C}$. This assembly supported a vacuum of 3×10^{-6} Torr. A specimen was initially subjected to a vacuum anneal at 800°C for 18 hr. It was then allowed to cool to room temperature by lowering the furnace from the reaction tube. Oxygen was then admitted to the assembly, the heated furnace raised around the reaction tube, and the growth of the oxide layer continuously recorded after waiting 5 min for the stabilization of temperature. Temperatures were controlled to $\pm 2^\circ\text{C}$.

RESULTS

The curves for growth of the nickel oxide layers on the three metal faces of different crystallographic orientation at temperatures of 500, 600, 700, and 800°C are shown in Figs. 1-3 ($1\ \text{mg O/cm}^2 = 6.3\ \mu$ of NiO). Two tests were completed at each temperature; the exposures extended to 100 and 50 hr when the curves were continuous and did not exhibit abrupt changes in slope caused by failure of the protective properties of a scale. These smooth curves for each face were reproducible within approximately $\pm 20\%$. For all exposures, the (100) nickel face exhibited curves of continuously decreasing slope and the oxide layer was completely adherent to the metal substrate. On the other hand, several oxidation curves for the (110) and (111) nickel faces showed abrupt changes in reaction rates, these changes being most frequent for the former crystal face. For the curves which were smooth, those for the (100) face exhibit the largest reaction rate at all temperatures. The oxidation rates for the (110) face were more rapid than those for the (111) face at 500 and 600°C while this order was reversed at 700 and 800°C . The minimum and maximum oxide thicknesses after

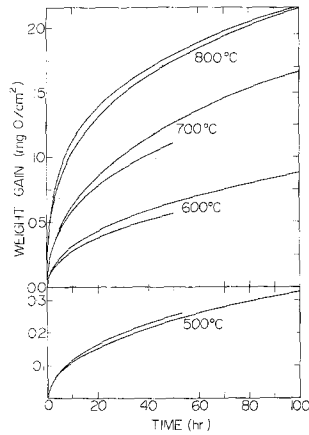


Fig. 1. Oxidation kinetics of the (100) nickel crystal face in oxygen at 400 Torr pressure.

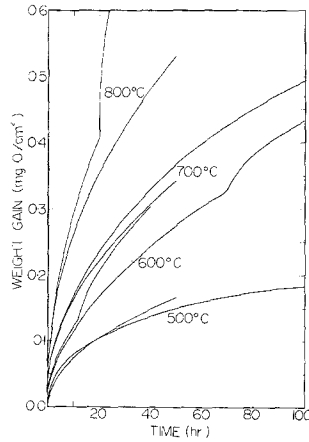


Fig. 2. Oxidation kinetics of the (110) nickel crystal face in oxygen at 400 Torr pressure.

100-hr exposures were 7000 \AA on the (111) nickel face exposed at 500°C and 14μ on the (100) face exposed at 800°C .

Several typical features of the scales were apparent upon their examination by scanning electron microscopy. As illustrated by the micrographs in Figs. 4–7, the scales were uniformly thick except where localized breakdown

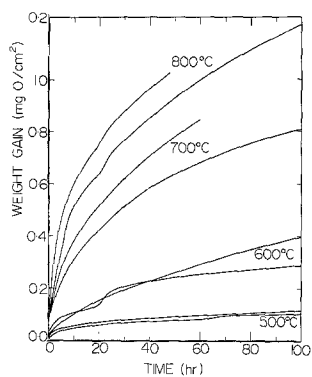


Fig. 3. Oxidation kinetics of the (111) nickel crystal face in oxygen at 400 Torr pressure.

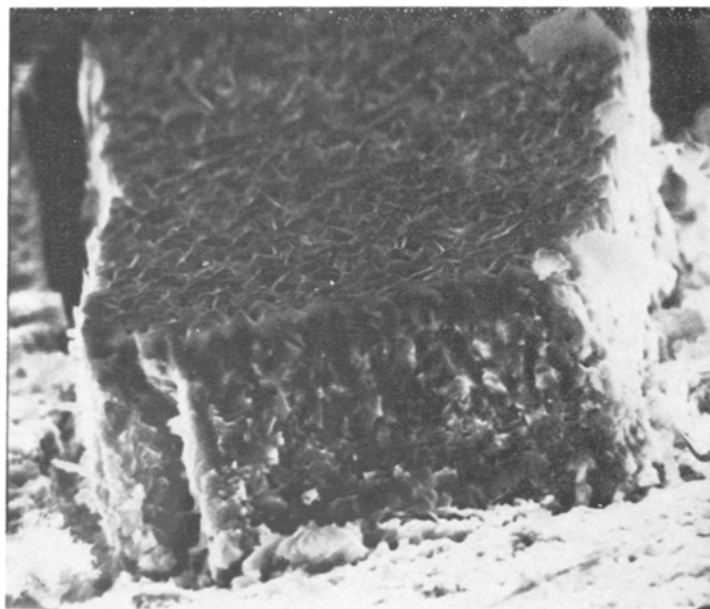


Fig. 4. Scanning electron micrograph of an oxide scale formed on the (100) nickel face at 800°C. Cross section formed by fracture. $\times 2000$.

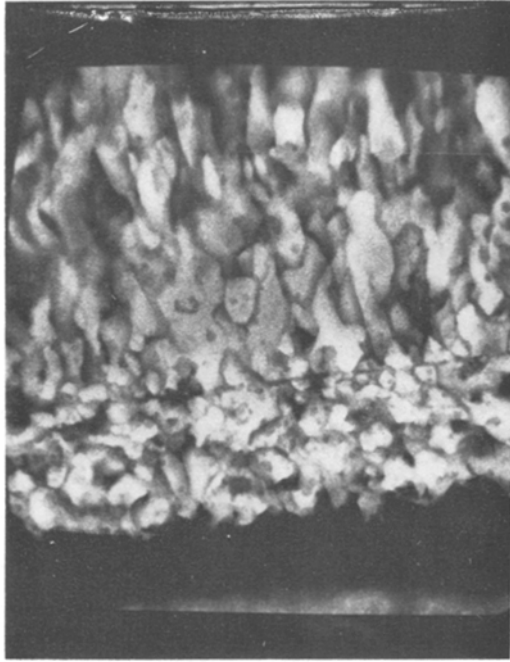


Fig. 5. Scanning electron micrograph of an oxide scale formed on the (100) nickel face at 800°C. Cross section prepared by metallographic polishing to 6 μ diamond and oxide then electrolytically etched in a 1:1:4 hydrofluoric acid–acetic acid–water solution. \times 3000.

had occurred by blistering and cracking of the oxide. They were polycrystalline; the grain size was in the order of only a few microns at 800°C. The micrographs also demonstrate that the grains were more columnar in the outermost region of a scale in comparison to grains of equi-axed shape in the innermost region near the metal interface. Those specimens which exhibited anomalous changes of reaction rate were blistered and cracked when examined after the exposure tests. To the eye, these specimens exhibited light green patches over the surface of the dark green oxide. This light oxide was cracked and even fragmented from the surface as illustrated in Fig. 6. Examination of cross sections as depicted in Fig. 7 demonstrated that these localized regions contained blisters. Apparently the protective property of a scale was destroyed by cracking of the oxide above a blister during the scaling reaction.

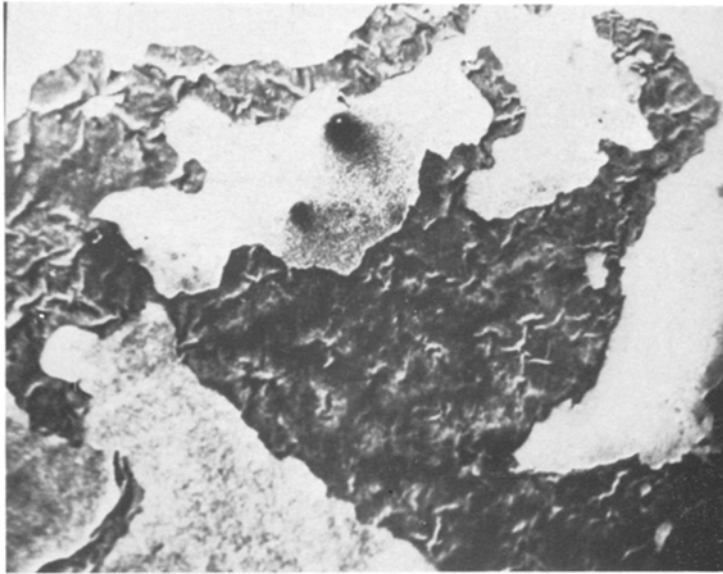


Fig. 6. Scanning electron micrograph of an outer scale surface area covered by oxide blister. Light and dark regions are areas showing oxide above and below blister. $\times 14$.



Fig. 7. Scanning electron micrograph of scale cross section at a blister after etching of oxide electrolytically in a 1:1:4 hydrofluoric acid-acetic acid-water solution. $\times 2000$.

DISCUSSION

Since nickel oxide is of NaCl structure, lattice diffusion is isotropic and structural parameters would not influence parabolic oxidation controlled solely by lattice diffusion of nickel across a scale. The oxidation curves demonstrate, however, that this condition is not satisfied as the (100) nickel face oxidized at rates more rapid than those for the (110) and (111) faces. Plots shown in Fig. 8 demonstrate this behavior. The oxidation curves for each metal face were placed in the parabolic form described by Eq. (1), $(\text{mg O}/\text{cm}^2)^2$ vs. t , and tangents to the curves determined by the finite differences method using a computer. These tangents are defined as an effective parabolic constant, $K(t)$, since this parameter is dependent upon both the time and scale thickness. This oxidation constant for the (100) face decreases with exposure time, the most rapid change occurring within the initial 25-hr period. The (110) and (111) faces exhibit similar behavior with the exception of runs at several temperatures where the effective parabolic constant initially increases before decreasing to lower values at exposures exceeding 50 hr. Thus structural properties of the oxide in the composite scale-metal system influence the oxidation rates of nickel at temperatures in the range 500–800°C. Elastic stress within a scale would not be expected to play a significant

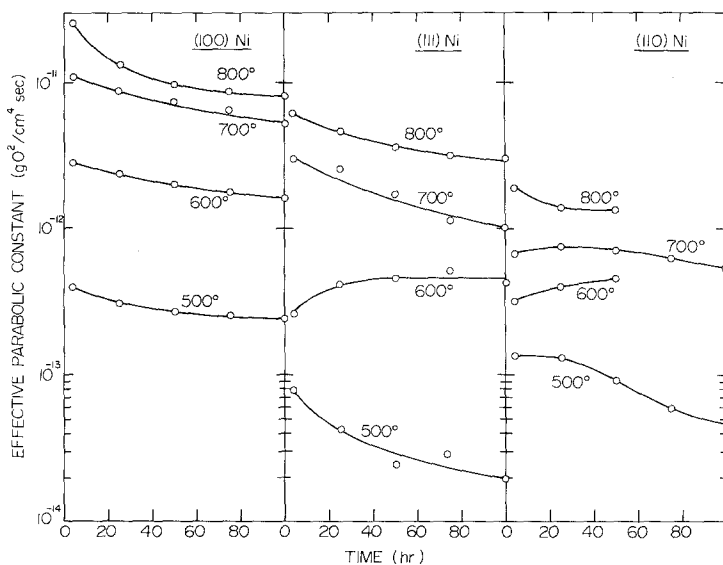


Fig. 8. Values of the effective parabolic oxidation constants, $K(t)$, versus exposure time determined from tangents to the oxidation curves in parabolic form for the (100), (110), and (111) nickel crystal faces.

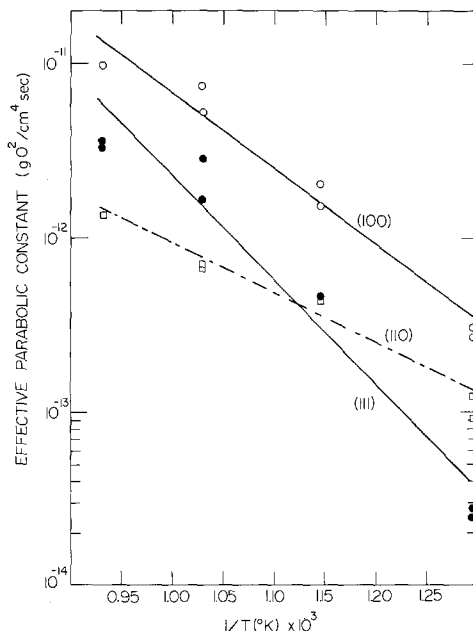


Fig. 9. Arrhenius plots of the effective parabolic oxidation constants, $K(t)$, for the (100), (110), and (111) nickel crystal faces exposed to oxygen for 50 hr.

role in this behavior since the oxide in films formed on several nickel crystal faces exhibit zero average strain.¹

Temperature coefficients of the effective parabolic oxidation constants also establish the inadequacy of considering scale growth by lattice diffusion only. Arrhenius plots of these constants for the metal faces are shown in Fig. 9. The values of the activation energy are 20, 13, and 28 kcal/g-atom for the (100), (110), and (111) nickel faces respectively. These temperature coefficients illustrate the relative oxidation rates of the (110) and (111) faces, the (111) face being the slowest oxidizing face at 500°C. The values of the activation energy, which may be compared to the value of 24 kcal/g-atom reported for the oxidation of polycrystalline nickel over the same temperature range, are but 0.3–0.5 of the activation energy for nickel self-diffusion in nickel oxide.^{6,7}

We have reported that the films formed at 500 and 600°C contain oxide crystallites with average sizes ranging from only a few hundred Angstroms at early exposures to values less than 5000 Å at long exposures.^{3,8} These films are highly oriented to the metal substrate by major epitaxial relationships. The oxide scales have now been shown to be polycrystalline and to

contain grains not exceeding a few microns in size even at the highest temperature investigated of 800°C. It is therefore imperative to consider the influence of the scale on nickel transport since the metal faces were oxidized at temperatures less than one-half the melting point of nickel oxide; at these temperatures recrystallization and grain growth proceed slowly and boundaries in polycrystalline oxide serve as effective short-circuit diffusion paths. A wide range of scale growth rates may, therefore, be expected for different metal faces because the degree of short-circuit diffusion would be determined by the densities and crystallographic orientations of boundaries within oriented oxide.

The plots shown in Fig. 10 for oxide growth in early exposure stages lend credence to the hypothesis that a modified parabolic equation is most appropriate for interpreting the reaction kinetics. Since the plots for the (100) nickel face and those for several of the other two faces obey parabolic relations, it would appear appropriate to account for changing rates with increasing exposure by a model wherein the effective parabolic constant exhibits a time dependence due to oxide structural properties. If lattice and boundary diffusion of metal both contribute to scale growth, the effective diffusion coefficient may be expressed as a weighted sum of the diffusion for lattice and boundary diffusion,

$$D_{\text{eff}} = D_L(1 - f) + D_B f \quad (2)$$

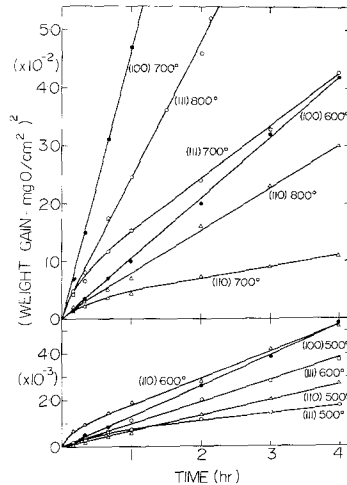


Fig. 10. Parabolic plots for the growth of nickel oxide layers during the initial 4 hr of exposure on the (100), (110), and (111) nickel crystal faces.

Utilizing the low gradient approximation for scale growth,

$$dx/dt = \Omega D_{\text{eff}}(\Delta c/x) \quad (3)$$

the modified equation becomes,

$$x^2 = 2\Omega D_L \Delta c \int_0^t (1 + f D_B/D_L) dt \quad (4)$$

In these equations, Ω is the volume of oxide per metal ion, f is the fraction of diffusion sites in the boundaries, Δc is the concentration difference across the scale. The boundary diffusion coefficient and the fraction of short-circuit sites would be dependent upon the structures of the scales on each metal crystal face and consequently account for the differences in the oxidation rates observed.

A model previously invoked to interpret oxide growth on polycrystalline nickel is used to interpret the results from the investigation.³ It was shown that the decrease in the density of short-circuit diffusion paths in the nickel oxide layer may occur by competitive growth of the oxide grains according to the following relationship,

$$D_t^2 - D_o^2 = Gt \quad (5)$$

where D_t is the mean diameter after time t , D_o is the initial grain diameter and G is the growth constant. If the oxide grains are considered as small cubes,

$$f(t) = 2d/D_t \quad (6)$$

where d is the boundary width. Upon substitution of (2), (5), and (6) into (3),

$$dx^2/dt = K_p \{1 + (D_B/D_L)[2d/(D_o^2 + Gt)]^{1/2}\} \quad (7)$$

In this expression, the parabolic oxidation constant for lattice diffusion of nickel by divalent vacancies and positive holes may be expressed in terms of the nickel self-diffusion coefficient,⁹

$$K_p = 2D_L \Omega \Delta c = 6D^* \quad (8)$$

Equation (7) may then be placed in the following form for graphical analysis,

$$1/(dx^2/dt - K_p)^2 = (D_o^2/A) + (Gt/A) \quad (9)$$

for $A = (2K_p D_B d)^2 / D_L$.

Oxide growth on the (100) and (111) metal faces is interpreted by this model since the effective parabolic oxidation constant continuously decreased with increasing exposure except for the (111) face at 600°C. These results

plotted according to Eq. (9) are shown in Figs. 11 and 12, and the corresponding fit of Eq. (7) to the results for the (100) face is shown in Fig. 13. It is thus seen that the modified parabolic equation accounts for the curves exhibiting decreasing parabolic slopes with increasing exposure. Moreover, parabolic oxidation governed by lattice diffusion does not come into effect even after exposures of 100 hr over the range 500–800°C.

This analysis substantiates the generalization that one must take into account short-circuit diffusion of a reactant in a scale when metals are exposed at temperatures less than one-half the melting point of their oxides which exhibit only small deviations from stoichiometry.^{10,11} The polycrystalline oxides at these temperatures exhibit short-circuit diffusion, a behavior to be found even when the oxides are formed as scales on metals. The present results demonstrate, however, that complicated morphological development and structural properties of scales influence their growth. Although a simple model accounted for several oxidation curves, the plots in Fig. 8 for the time dependence of the effective parabolic oxidation constants show that the structurally dependent parameters, the boundary diffusion coefficient and the fraction of diffusion sites at boundaries, may not be related to the oxide structures in any simple manner. It is also possible that other line defects, such as dislocations within the oxide grains, may play a role in the diffusion mechanism.

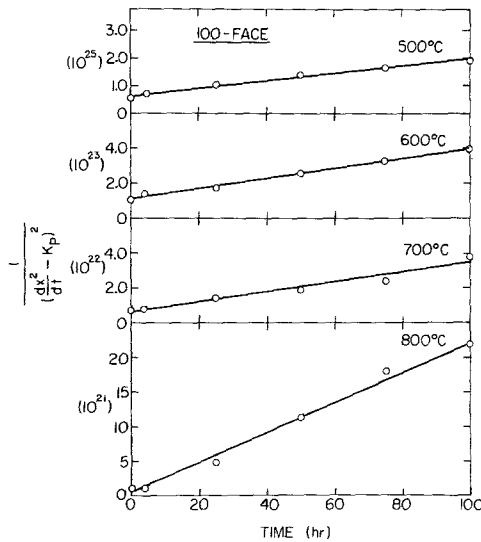


Fig. 11. Plots of the effective parabolic oxidation constants, $K(t)$, for the (100) nickel crystal face according to Eq. (9).

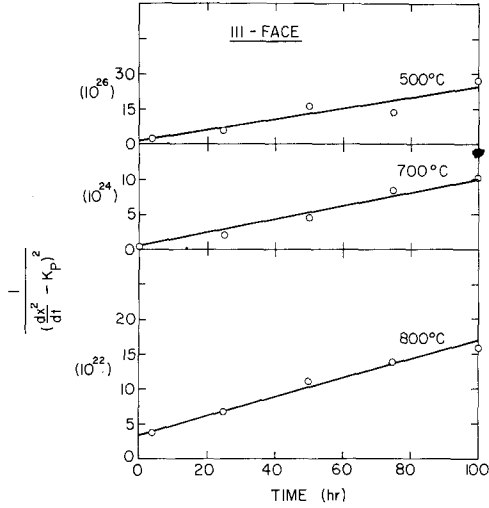


Fig. 12. Plots of the effective parabolic oxidation constants, $K(t)$, for the (111) nickel crystal face according to Eq. (9).

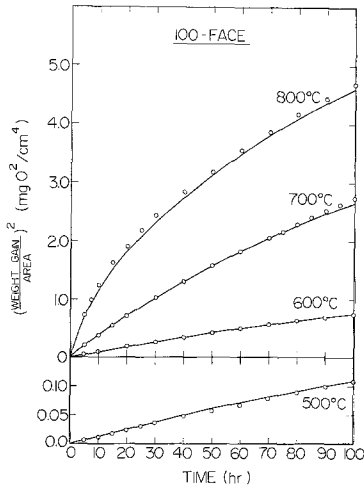


Fig. 13. The experimental results and the curve (7) calculated by Eq. (7) for the growth of the nickel oxide layers on the (100) nickel crystal face in parabolic form.

Oxidation runs were carried out under the same conditions for each metal face by exposing a vacuum-annealed specimen to oxygen at room temperature before rapidly heating it to the reaction temperature. Reproducible kinetics were obtained under these arbitrarily selected conditions except when scales fractured by a blistering mechanism. With respect to the faces, it was previously demonstrated that electropolished specimens do not exhibit residual oxide or facets when subjected to vacuum anneals of 10^{-6} Torr or 10^{-10} Torr at 700°C .⁸ The surfaces after the former anneal, nevertheless, are "dirty" and the oxidation rates of the individual crystal faces must be sensitive to the initial surface treatment. For example, the oxidation rates of the (100) face were found to be more rapid than those for the (110) and (111) faces whereas nickel crystals subjected to hydrogen anneals oxidize at decreasing rates in the order (110), (100), (111) at 500 and 600°C .¹ Treatment of specimens by hydrogen is known to influence the rates of oxide growth during nucleation and film formation.¹² Hence, morphological development of oriented oxide which influences the densities and types of boundaries in a scale on an individual metal crystal face and, in turn, its oxidation rate must presently be regarded as sensitive to undefined relations between crystallographic and impurity properties of the metal surfaces.

CONCLUSIONS

The results from this investigation have demonstrated that growth of nickel oxide on different nickel crystal faces during long exposures at temperatures in the range $500\text{--}800^{\circ}\text{C}$ does not proceed by parabolic kinetics governed by lattice diffusion of nickel through the superficial scales. Under the conditions for preparation and oxidation of the metal crystal faces, the (100) face oxidized more rapidly than the (110) and (111) faces. These latter faces oxidized at relative rates dependent upon temperature. The oxide layers were polycrystalline; the grains were in the few hundred Angstrom to micron size range. The temperature coefficients of oxidation, the scale morphologies, and the fit of several oxidation curves to a modified parabolic oxidation equation were consistent with the hypothesis that oxide growth proceeded by short-circuit and lattice diffusion of nickel through nickel oxide when the scales remained adherent to the metal substrate.

ACKNOWLEDGMENTS

The authors are indebted to Dr. J. D. Embury for helpful discussions. One author (N. N. Khoi) wishes to express his appreciation of the award of an Ontario Graduate Fellowship.

REFERENCES

1. J. V. Cathcart, G. F. Petersen, and C. J. Sparks, Jr., *J. Electrochem. Soc.* **116**, 664 (1969).
2. J. M. Perrow, W. W. Smeltzer, and R. K. Ham, *Acta Met.* **15**, 577 (1967).
3. J. M. Perrow, W. W. Smeltzer, and J. D. Embury, *Acta Met.* **16**, 1209 (1968).
4. E. A. Gulbransen and K. F. Andrew, *J. Electrochem. Soc.* **101**, 128 (1954).
5. J. J. Van der Broeck and J. L. Meijering, *Acta Met.* **16**, 375 (1968).
6. L. Berry and J. Paidassi, *Compt. Rend. Acad. Sci. Paris* **262**, 1353 (1966).
7. M. L. Volpe and J. Reddy, *J. Chem. Phys.* **53**, 1117 (1970).
8. T. Homma, N. N. Khei, W. W. Smeltzer, and J. D. Embury, *Oxidation Metals* **3**, 463 (1971).
9. N. F. Mott and R. W. Gurney, *Electronic Processes in Ionic Crystals* (Clarendon Press, Oxford, 1948).
10. A. Madeyski, D. J. Poulton, and W. W. Smeltzer, *Acta Met.* **17**, 579 (1969).
11. W. W. Smeltzer, *Oxidation of Metals and Alloys*, ASM monograph (1971), p. 115.
12. K. R. Lawless, F. W. Young, Jr., and A. T. Gwathmey, *J. Chim. Phys.* **53**, 667 (1956).